Tropical Journal of Pharmaceutical Research November 2026; 25 (11): 1573-1587
ISSN: 1596-5996 (print); 1596-9827 (electronic)

Available online at http://www.tjpr.org
https://dx.doi.org/10.4314/tjpr.v25i11.11

Original Research Article

Synthesis and characterization of new heterocyclic compounds with potential antitumor activity and their immobilization on copolymer supports

Nidal Hassoun Thamer*, Mohammed Ali Mutar
Department of Chemistry, College of Sciences, University of Al Qadisiyah, Iraq

For correspondence:* ***Email:* *nidal.hassoun@qu.edu.iq*

Sent for review: 25 July 2026 *Revised accepted: 14 November 2026*

Abstract

Purpose: *To investigate the in vitro cytotoxic activity of synthesized novel heterocyclic compounds and methacrylic acid -co-itaconic anhydride (MAA-co-IAN) copolymer conjugates against human colorectal cancer cells.*
Methods: *The physical properties, including colour, melting point, and elemental (CHNS) analysis, of synthesized compounds and copolymers were determined. Chemical structures were characterized using Fourier-transform infrared spectroscopy (FTIR), proton nuclear magnetic resonance (^{1}H NMR), and carbon-13 carbon^{13} nuclear magnetic resonance (^{13}C NMR). Cytotoxic activity was evaluated against human colorectal carcinoma (HCT-116) and normal human dermal fibroblast (HdFn) cell lines using the 3-(4,5-dimethylthiazol-2-yl)-2,5-diphenyltetrazolium bromide (MTT) assay, and the half-maximal inhibitory concentration (IC_{50}) was determined at 24, 48, and 72 h after exposure.*
Results: *Spectroscopic analyses confirmed successful synthesis of target heterocyclic compounds and their polymer-supported derivatives. These MAA-co-IAN polymer conjugates exhibited concentration- and time-dependent cytotoxic activity against HCT-116 cells. HCT-116, IC_{50} rose from 38.16 µg/mL (48 h) to 50.62 µg/mL (72 h). At 24 h, the IC_{50} value for HCT-116 was 34.4. The compounds demonstrated greater inhibitory activity against the cancer cell line compared to the normal HdFn cell line, indicating selective cytotoxicity. Among the synthesized derivatives, differences in anticancer activity were observed, suggesting that structural modifications influenced biological performance.*
Conclusion: *The synthesized compounds and copolymer conjugates showed selective cytotoxic activity against HCT-116 cells, demonstrating their potential as promising anticancer agents.*

Keywords: *Anticancer, Copolymer, Cytotoxicity, Heterocyclic compounds, Methacrylic acid-itaconic anhydride copolymer*

This is an Open Access article that uses a funding model which does not charge readers or their institutions for access and distributed under the terms of the Creative Commons Attribution License (http://creativecommons.org/licenses/by/4.0) and the Budapest Open Access Initiative (http://www.budapestopenaccessinitiative.org/read), which permit unrestricted use, distribution, and reproduction in any medium, provided the original work is properly credited.

Tropical Journal of Pharmaceutical Research is indexed by Scopus, Chemical Abstracts, Embase, Index Copernicus, EBSCO, African Index Medicus, JournalSeek, Directory of Open Access Journals (DOAJ), African Journal Online, Bioline International, Open-J-Gate and Pharmacy Abstracts

INTRODUCTION

Heterocyclic compounds are giants among organic-anchored chemical classes, and their influence on human evolution has been enormous. Vitamins B1, B2, and C, as well as glucose and deoxyribonucleic acid (DNA), are examples of heterocyclic compounds essential to human metabolic processes [1]. Due to their remarkable heat endurance, heterocyclic polymers have widespread usage in many industries, including aviation. A diverse array of heterocyclic polymers with specific properties has been developed and manufactured as a result of advancements in science, technology,

© 2026 The authors. This work is licensed under the Creative Commons Attribution 4.0 International License

engineering and mathematics (STEM) fields. The distinctive thermal, mechanical, and photophysical characteristics displayed by heterocyclic polymers (as a result of the electronic effect) have led to their incorporation into numerous biological-based materials, organic photovoltaics, light-emitting diodes, and photophysical applications [2].

Various immobilization approaches are used to improve the quality of bioactive compounds, enhance their stability and release behaviour, and reduce toxicity. In medicinal chemistry, polymer-supported heterocyclic derivatives have emerged as promising candidates for the development of targeted therapeutic systems due to enhanced interaction with biological environments and drug delivery efficiency. Functional polymer science is an interdisciplinary field encompassing environmental science, biology, materials science, polymer chemistry, and more. This field is still in its infancy, having only been established in the 1960s [2].

Although heterocyclic polymers offer several potential applications, their synthesis is challenging. Using reactive heterocyclic monomers and immediately connecting all the altered heterocycles to the polymer backbones is a typical synthesis technique. The lengthy reaction time, challenging polymerization conditions, problems with multiple substituent incorporation, and high cost of heterocyclic monomers are some of the common obstacles to this synthesis approach. Acetylenic polymers, on the other hand, are composed of triple-bond building blocks, and the main chains of these polymers have fused aromatic rings, electrically unsaturated double bonds, or heterocyclic units [3].

Functional groups and macromolecular properties of reactive functional groups on synthetic polymers are now the focus of research and application. There is currently considerable interest in functional polymers with specialized properties, such as materials with antimicrobial properties [4]. Thiosemicarbazones and their metal complexes are recognized to possess several biological activities, including antifungal, antimalarial, and antiviral properties. There is extensive experience with thioacetazone, formerly known as acetamidobenzaldehyde thiosemicarbazone, in the treatment of tuberculosis [5]. The biological activity of these compounds depends on several factors, including the geometry of the thiosemicarbazone group, orientation of attachment to the heteroaromatic ring, and nature of the ring itself. Triazole, thiosemicarbazone, imidazole, and benzothiazole derivatives have been reported to possess antimicrobial, antifungal, anthelmintic, pesticidal, and herbicidal properties [6].

Other nucleophilic compounds may be able to open the anhydride ring in anhydride acid-based copolymers, resulting in the formation of new molecules with potential biological activity. Several systems have been reported in the literature following the use of heterocyclic compounds to open the anhydride ring of anhydride copolymers with certain vinyl monomers, particularly methacrylate [7]. This study investigated the *in vitro* cytotoxic activity of synthesized novel heterocyclic compounds and methacrylic acid-co-itaconic anhydride (MAA-co-IAN) copolymer conjugates against human colorectal cancer cells.

METHODS

Synthesis of Compound 1: 3-amino-5-(5-(1,3-dioxo-1,3-dihydroisobenzofuran-5-carbonyl)-3-methylene-1-oxoisoindolin-2-yl)-4,5-dihydro-1,3,4-thiadiazol-2-yl benzoic acid

Compound 1 was synthesized by combining glacial acetic acid and pyridine (3:2, v/v; 80 mL), 6.8 mmoles of 3,3′,4,4′-benzophenone tetracarboxylic dianhydride (Sigma-Aldrich, Germany) and 21.2 mmoles of N-(5-aminophthaloyl) thiosemicarbazide (synthesized in our laboratory) in a 250 mL round-bottom flask. The mixture was stirred at room temperature for 2 h, refluxed at 60 °C for 1 h, cooled, and filtered. The precipitate was washed with distilled water and dried in a K-VO27 vacuum oven (K & K Scientific Supplies, South Korea). This process was repeated until 4.2 g yield was obtained as sufficient amount of product required to proceed with the subsequent conjugation of the compound with the copolymer.

Synthesis of Compound 2: 1,1′-(dispiro[tetrazole-5,2′-indoline-3′,5″-tetrazol]-1,1″(4H,4″H)-diyl)bis(thiourea)

Compound 2 was synthesized by reacting 0.01 M isatin (Sigma-Aldrich, Germany) with 0.01 M 2,2′-((Z)-indoline-2,3-diylidene)bis(hydrazine-1-carbothioamide) in 10 mL tetrahydrofuran (THF; Merck KGaA, Germany) enriched with 0.02 M sodium azide (Sigma-Aldrich, Germany). The mixture was heated at 60–70 °C for 10 h and allowed to cool to room temperature. The precipitate was collected by filtration and purified using absolute ethanol (Scharlau**,** Spain).

Synthesis of Compound 3: 3-((3-(4-aminophenoxy)phenyl)amino)-3,4-dihydro-2H-thiazolo[3,2-a][1,3,5]triazin-6(7H)-one

Compound 3 was synthesized by combining 0.024 M formalin with 0.92 g of 2-iminothiazolidin-4-one and 1 g of 3,4-diaminodiphenyl ether (Sigma-Aldrich, Germany) under continuous stirring at 0–5 °C. The mixture was stirred for 15 min, after which 20 mL of warm dry benzene (30–40 °C; Merck KGaA, Germany) was added in four equal portions with continuous stirring.

The benzene layer was separated, dried over anhydrous magnesium sulfate, and concentrated until approximately one-fifth of the original volume remained. The concentrated reaction mixture was allowed to cool to room temperature. The precipitate was filtered, washed and dried.

Synthesis of copolymer (methacrylic acid-co-itaconic anhydride, MAA-co-IAN)

Methacrylic acid (MAA; Sigma-Aldrich, Germany) was combined with itaconic anhydride (IAN; Sigma-Aldrich, Germany) in a 250 mL round-bottom flask and maintained under a nitrogen atmosphere with continuous stirring at room temperature for 30 min.

Polymerization conditions include MAA (5 g), IAN (5 g), and 0.1 g of 1-hydroxycyclohexyl phenyl ketone at room temperature, for 30 min, under nitrogen. Ultraviolet radiation was used at wavelength of 365 nm.

Copolymer isolation

The copolymer was precipitated using a non-solvent in which it was insoluble. The precipitate was separated by filtration and washed to remove residual monomers and initiator.

The copolymer was dried to obtain the final product. Throughout the copolymer production, 1-hydroxycyclohexyl phenyl ketone (0.1 g; Sigma-Aldrich, Germany) was used as an initiator.

Synthesis of Compound 1 conjugate: MAA-co-IAN

The MAA-co-IAN copolymer (0.5 M) was dissolved in 20 mL absolute ethanol. Thereafter, 0.5 M of Compound 1 was gradually added and stirred continuously at room temperature for 1 h. The polymer conjugate formed was filtered, washed with ether, recrystallized from absolute ethanol and dried.

Synthesis of Compound 2 conjugate

Compound 2 (0.5 M) was dissolved in 20 mL absolute ethanol with 0.5 M MAA-co-IAN under continuous stirring at room temperature. The precipitate was filtered, washed with ether, and recrystallized from ethanol.

Synthesis of Compound 3 conjugate

The 0.5 M MAA-co-IAN was dissolved with 0.5 M of Compound 3 in 20 mL of pure ethanol while stirring at room temperature for 1 h. The precipitate was filtered, washed with ether, and recrystallized from ethanol.

Structural characterization of synthesized compounds and polymer conjugates

The colour, yield, and melting point of the synthesized compounds were determined. The compounds were characterized by Fourier transform infrared (FTIR) spectroscopy using a Bruker FT-IR-8400^{s} spectrophotometer (Bruker Company, Germany). Proton (^{1}H) and Carbon-13 (^{13}C) nuclear magnetic resonance (NMR) spectra were acquired on a Bruker UltraShield 500 MHz spectrometer (Bruker, Switzerland) using dimethyl sulfoxide-d^{6} (DMSO-d^{6}) as the solvent. Elemental analysis was performed to confirm their chemical structure and purity using a Thermo Fisher Flash 2000 CHNS/O Elemental Analyzer (Thermo Fisher Scientific, USA).

Preparation of reagents

Preparation of phosphate-buffered saline solution (PBS)

Sodium chloride (8 g), potassium chloride (0.2 g), potassium dihydrogen phosphate (KH_2PO_4; 0.24 g) and disodium hydrogen phosphate (Na_2HPO_4; 1.44 g). The salts were dissolved in 800 mL of distilled water, and the final volume was adjusted to 1000 mL with additional distilled water.

Preparation of trypsin solution

Trypsin (1 g) was dissolved in 100 mL PBS, and the slurry was sterilized using a Millipore membrane filter (0.22 µm).

Preparation of ethylenediaminetetraacetic acid (EDTA) solution

Ethylenediaminetetraacetic acid (1 g) was dissolved in 100 mL of PBS to make a 1 % solution, which was sterilized using an autoclave.

Preparation of trypsin-EDTA solution

Trypsin–EDTA solution was prepared by mixing 20 mL of trypsin solution with 10 mL of chelating agent (EDTA) solution and 370 mL of phosphate-buffered saline (PBS), yielding a final volume of 400 mL. The final concentrations of trypsin and EDTA were 0.05 and 0.025 %, respectively. The prepared solution was stored at 4 °C until use.

Roswell Park Memorial Institute (RPMI)-1640 medium

The RPMI-1640 medium was supplemented with 4-(2-hydroxyethyl)-1-piperazineethanesulfonic acid (HEPES), L-glutamine, penicillin (10^3 IU), streptomycin (0.001 g), 1 % sodium bicarbonate, and 15 % fetal bovine serum (FBS) and was used for cell culture, while serum-free RPMI-1640 served as the serum-free medium.

Cell lines and assay procedure

The human colorectal adenocarcinoma cell line used for the cytotoxicity assay was obtained from the Centre for Natural Product Research and Drug Discovery, Department of Pharmacology, Faculty of Medicine, University of Malaya, Malaysia. The cell line was originally established from a patient diagnosed with colorectal adenocarcinoma and maintained according to standard cell culture procedures prior to use. Cytotoxic activity of the compounds against human colorectal carcinoma (HCT116) and human malignant melanoma (A375) cell lines and HDFn (normal cell line) was evaluated using the MTT assay following a previously reported method [8].

Cell line culture and maintenance

The HCT116, A375, and normal human dermal fibroblast (HdFn) cell lines were cultured in RPMI-1640 medium and maintained at 37 °C in a humidified atmosphere containing 5 % CO_2 until 70–80 % confluence was reached. Thereafter, the adherent cells were washed twice with PBS. Trypsin-EDTA (3 mL) solution was added to ensure that the monolayer was covered completely and the plate was incubated at 37 °C for 2 min until the cells detached from the surface of the plate. Trypsin activity was stopped after adding RPMI-1640 medium and the cells were then transferred into fresh RPMI culture medium. Plates were incubated in an incubator containing 5 % CO_2. Cell density was determined using a haemocytometer and adjusted to the required concentration using Eq 1.

Total cell count/mL = cell count × dilution factor (sample volume) × 10^4 …….. (1)

3-(4,5-dimethylthiazol-2-yl)-2,5-diphenyltetrazolium bromide (MTT) assay

The MTT kit containing 3-(4,5-dimethylthiazol-2-yl)-2,5-diphenyltetrazolium bromide (Intron Biotech, Korea) was used in this study. Cancer cells were cultured in 96-well plates with 200 µL of culture medium per well. The plates were incubated at 37 °C for 24 h. After incubation, the medium was discarded, followed by a two–fold serial dilution of test compounds (25, 50, 100, 200 and 400 µg/mL), and 200 µL from each concentration was added to the wells.

Triplicates determinations were performed at each concentration and control and the plates were incubated in a CO_2 incubator at 37 °C, 5 % CO_2 for 24 h. Thereafter, 10 µL of MTT solution was added to each well and the plates were incubated in CO_2 incubator for 4 h in the dark. The medium was carefully removed and 100 µL of solubilization solution was added into each well and incubated for 5 min. Absorbance was measured at 575 nm using an enzyme-linked immunosorbent assay (ELISA) microplate reader. The data was subjected to statistical analysis in order to calculate the concentration of compounds required to cause 50 % reduction in cell viability for each cell line (IC_{50}).

Statistical analysis

Data were analysed using Statistical Package for the Social Sciences (SPSS version 31.0.0.0; IBM Corp., Armonk, NY, USA). Data were expressed as mean ± standard deviation (SD), and GraphPad Prism version 10 (GraphPad Software Incorporated, La Jolla, California) was used to determine the IC_{50} values.

Data were analyzed using the Statistical Package for the Social Sciences (SPSS version 31.0.0.0, IBM Corp., Armonk, NY, USA). Data were expressed as mean ± standard deviation (SD), and GraphPad Prism version 10 (GraphPad Software, LLC, Boston, MA, USA) was used to determine the IC_{50} values.

RESULTS

Physicochemical properties

Compound 1 was brown in colour, compound 2 was an orange crystalline solid, and compound 3 was also brown, with yields of 93, 92, and 94 %, respectively (Table 1; Figure 1).

Table 1: Physicochemical properties

Formula		m.p/°C	Weight (g)	Yield (%)
Compound 1				
$C_{26}H_{12}N_4O_8S$	Brown	-	4.2	93
Compound 2				
$C_{10}H_{13}N_{13}S_2$	Orange	201-204	3.9	92
Compound 3				
$C_{17}H_{17}N_5O_2S$	Brown	240-243	1.8	94

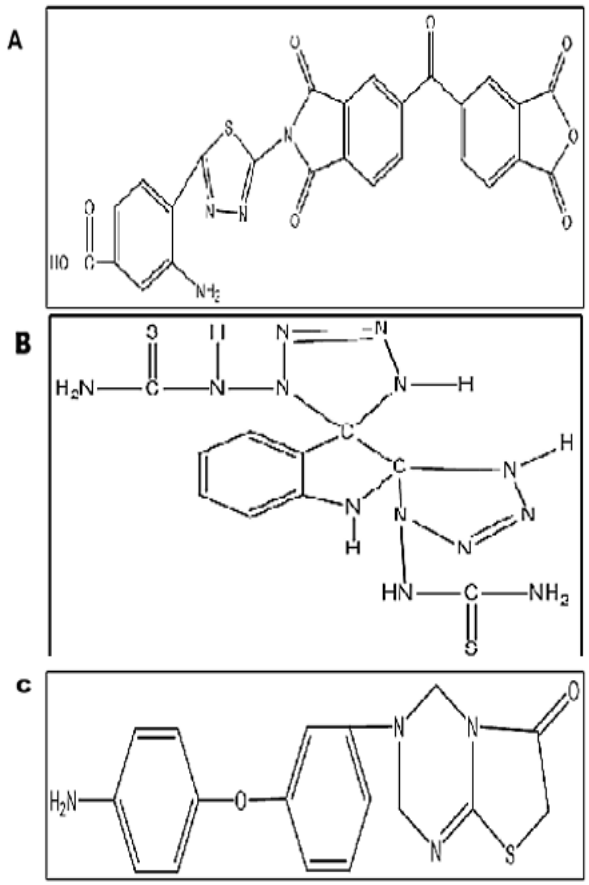

Figure 1: Structural configuration of synthesized compounds. A (Compound 1), B (Compound 2), C (Compound 3)

Elemental analysis

The results showed that % C was higher in all the compounds compared to % H, % N, % O, and % S (Table 2).

FTIR spectrum of synthesized compounds

The FTIR spectrum indicated an absorption band at 3456 cm^{-1} assigned to NH_2 overlapping with the –OH group, absorption band at 3074 cm^{-1} assigned to C-H (aromatic), absorption band at 1539 cm^{-1} assigned to C=C (aromatic), absorption band at 1635 cm^{-1} assigned to C=O (amide), absorption band at 1714 cm^{-1} assigned to C=O (carboxylic acid), absorption band at 1163 cm^{-1} assigned to C-N (Compound 1). There was a simultaneous presence of characteristic amino, carbonyl, imine, and aromatic absorption bands (Compounds 2 and 3; Figure 12).

^{1}H NMR spectroscopy of Compound 1

Multiplet signals occurred at (7.3 - 8.1 ppm) assigned to (9H, phenyl ring), a singlet at (8.9 ppm) assigned to (1H, OH), and a singlet at (3.4 ppm) assigned to $–NH_2$ (Compound 1). The major signal at δ 2.5 ppm was characteristic of DMSO-d_6 as solvent, singlets at (6.7 - 8.3 δ ppm) assigned to (4H, phenyl ring), a singlet at (3.5 ppm) assigned to $–NH_2$ (Compound 2). Furthermore, singlets occurred at (7.1 - 7.4 δ ppm) assigned to (8H, phenyl ring), a singlet at (3.4 ppm) assigned to $–NH_2$, and a singlet at (2.5 δ ppm) assigned to CH_2 (Compound 3; Figure 3).

^{13}C NMR spectroscopy of synthesized compounds

Signals of olefinic and aromatic carbons appeared in the third region between 123 and 134 ppm, signals related to C-S at 56 ppm, signals related to C=N at 166 ppm, signal related to C-N at 64 ppm, signal related to C=O at 173 ppm (Compound 1).

Table 2: Data of elemental analysis of synthesized compounds (calculated vs. found values)

Item	C (%)	H (%)	N (%)	O (%)	S (%)
Compound 1: $C_{26}H_{12}N_4O_8S$					
Calculated	57.78	2.24	10.37	23.68	5.93
Found	57.98	2.34	10.47	23.78	6.13
Compound 2: $C_{10}H_{13}N_{13}S_2$					
Calculated	31.66	3.45	47.99	-	16.90
Found	31.96	3.65	48.14	-	17.1
Compound 3: C17H17N5O2S					
Calculated	57.46	4.78	19.71	9.04	9.01
Found	57.76	5.08	20.01	9.34	9.31

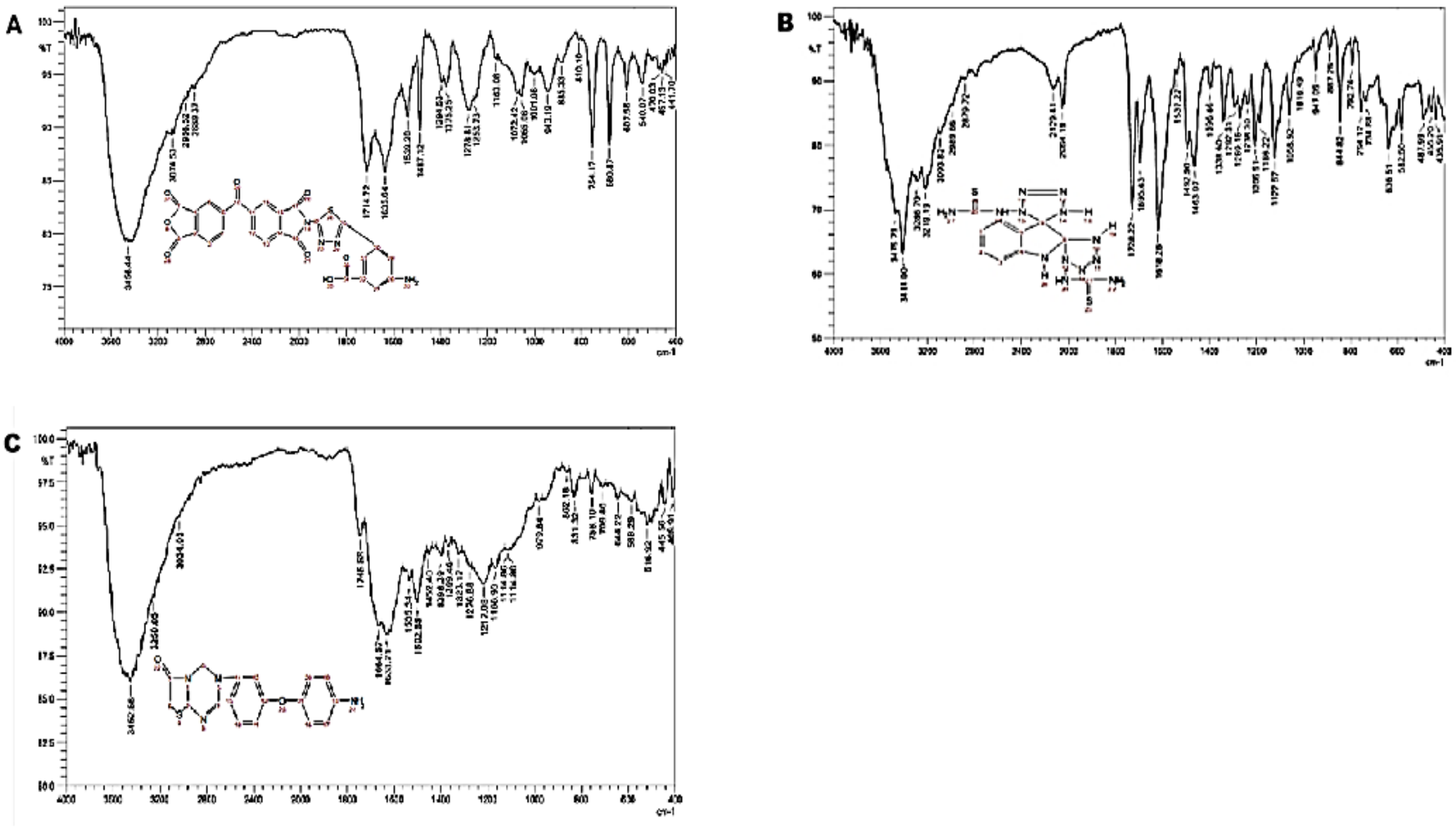

Figure 2: FTIR spectrum of the synthesized compounds. A (Compound 1), B (Compound 2), C (Compound 3)

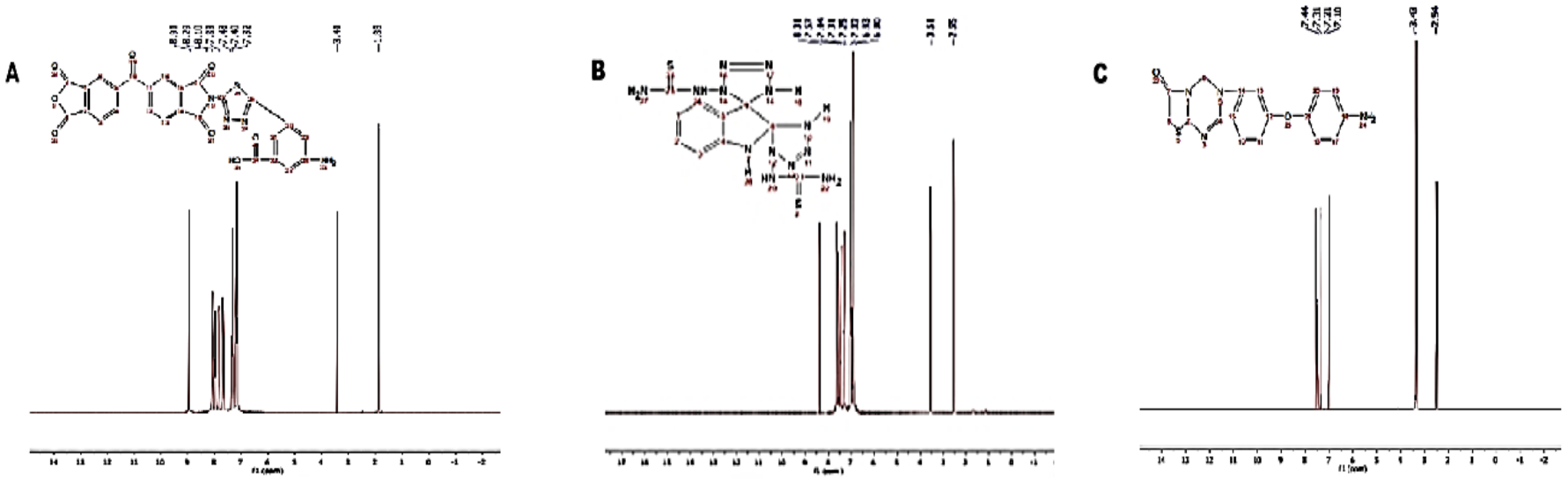

Figure 3: ^{1}H NMR spectrum of synthesized compounds. A (Compound 1), B (Compound 2), C (Compound 3)

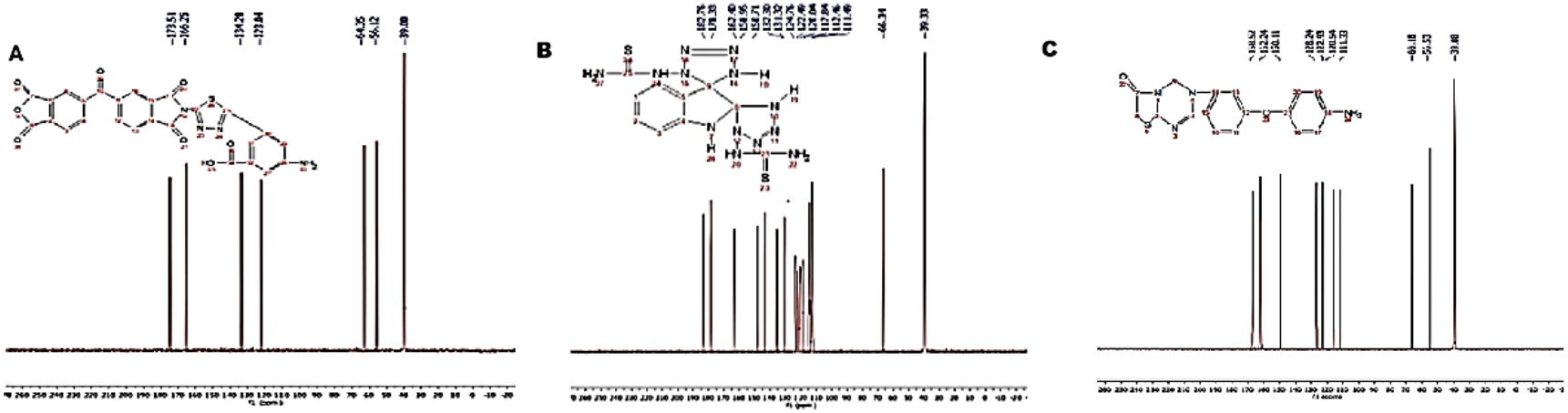

Figure 4: ^{13}C-NMR spectra of synthesized compounds. A (Compound 1), B (Compound 2), C (Compound 3)

Table 3: Physicochemical characteristics of copolymer MAA-co-IAN and conjugates

Formula	Colour	m.p/°C	Weight (m)	Yield (%)
Copolymer MAA-co-IAN				
$C_{15}H_{24}O_5$	White	-	10	99
MAA-co-IAN-compound 1 conjugate				
$C_{37}H_{28}N_4O_{13}S$	Light brown	-	0.9	90
MAA-co-IAN-compound 2 conjugate				
$C_{21}H_{29}N_{13}O_5S_2$	Light orange	-	0.9	90
MAA-co-IAN-compound 3 conjugate				
$C_{28}H_{33}N_5O_7S$	Light brown	-	0.9	90

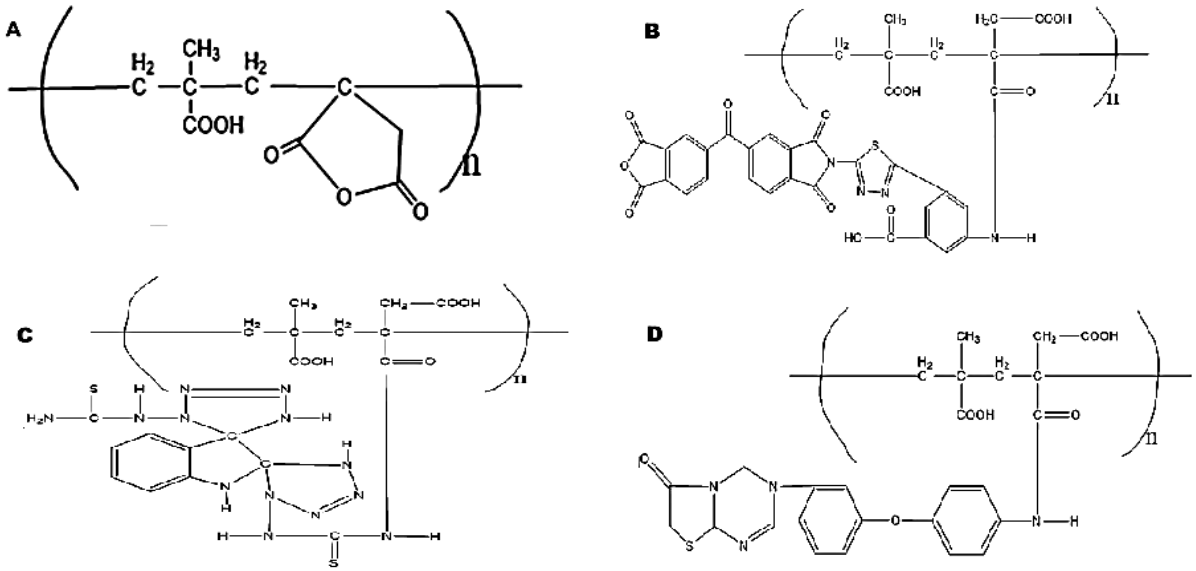

Figure 5: Structural configuration of copolymer MAA-co-IAN (A), MAA-co-IAN-compound 1 conjugate (B), MAA-co-IAN-compound 2 conjugate (C), MAA-co-IAN-compound 3 conjugate (D)

Signals of olefinic and aromatic carbons appeared in the third region between 111 and 132 ppm, signal related to C=N at 150–162 ppm, signal related to C-N at 66 ppm, signal related to C=S at 178–182 ppm (Compound 2). Signals of olefinic and aromatic carbons appeared in the third region between 111 and 128 ppm, signal related to C=N at 150162 ppm, signal related to C-N at 66 ppm, signal related to C-S at 56 ppm, signal related to C=O at 168 ppm (Compound 3; Figure 4).

Physicochemical characteristics of copolymer MAA-co-IAN and conjugates

The copolymer was white in colour, while the conjugates were light brown (compound conjugates 1 and 3) and light orange (compound conjugate 2; Table 3; Figure 5).

FTIR spectrum of copolymer MAA-co-IAN and conjugates

The spectrum showed absorption bands at 3411 cm^{-1} for OH, 3107 cm^{-1} for C-H (heterocyclic ring), 2929 cm^{-1} for CH_2 (aliphatic), 1708 $cm^{-1}$for C=O (ester), 1699 cm^{-1} for C=O (carboxylic acid), 1309 cm^{-1} for CH_3, and 1166 cm^{-1} for C-O (copolymer MAA-co-IAN; Figure 6).

The FTIR spectrum of syntheses of copolymer (1; MAA-Co-IAN) with 3-amino-5-(5-(5-(1, 3-dioxo-1, 3-dihydroisobenzofuran-5-carbonyl) -3-methylene-1-oxoisoindolin-2-yl) -4, 5-dihydro-1, 3, 4-thiadiazol-2-yl) benzoic acid is shown in Figure 6 B. The absorption band are assigned at 3419 cm^{-1} to -OH overlapping with NH, 3070 to C-H (aromatic), 2981 to C-H (aromatic), 1541 cm^{-1} to C-H and C=N, 1489 cm^{-1} to C=C (aromatic), 1637 cm^{-1} to C=O (amide), 1712 cm^{-1} to C=O (carboxylic acid), 1178 cm^{-1} to C-N, and 1390 cm^{-1} to CH_3.

The FTIR spectrum synthesis of copolymer (2; MAA-Co-IAN) with 1, 1'-(dispiro[tetrazole-5, 2'-indoline-3', 5''-tetrazol]-1, 1''(4H, 4''H) -diyl) bis(thiourea) is shown in Figure 6 C. It assigns absorption band at 3415 cm^{-1} to –OH and 3213 cm^{-1} to–NH, 3174 cm^{-1} to C-H (aromatic), 2987 cm^{-1} to C-H (aliphatic), 1290 cm^{-1} to C=S, 1462 cm^{-1} to C=C (phenyl ring), 1056 cm^{-1} to C-N, 1056 cm^{-1} to C-O, 1728 cm^{-1} to C=O (acid), 1695 cm^{-1} to C=O (amide), 1618 cm^{-1} to C=N, 1396 cm^{-1} to CH_3, and 1492 cm^{-1} to N=N.

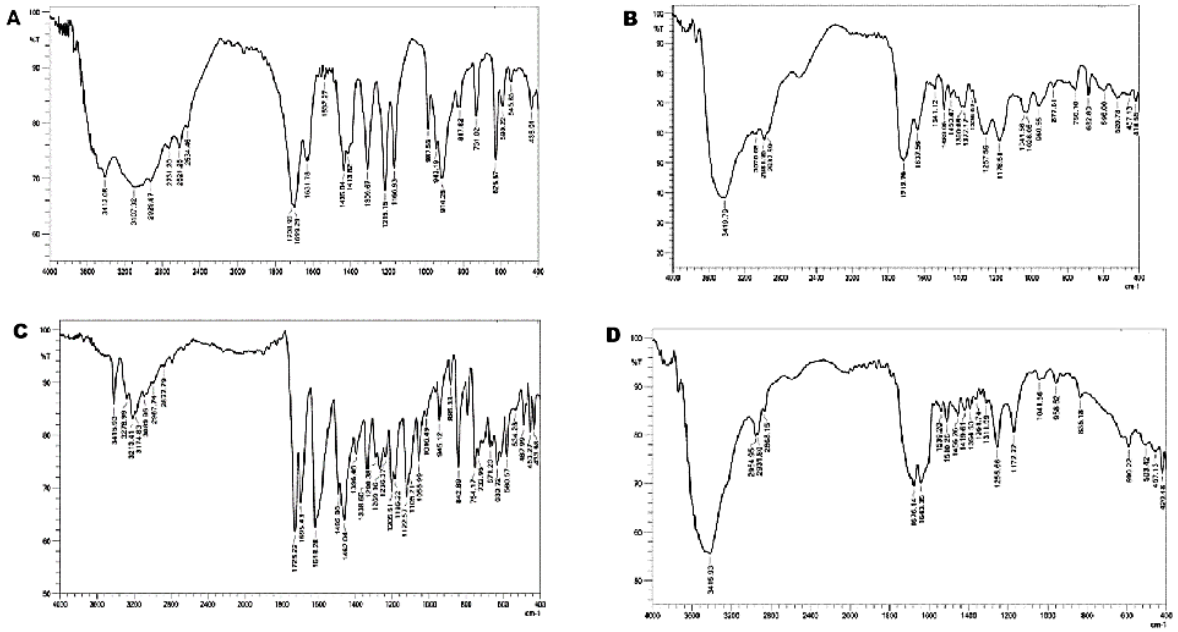

Figure 6: FTIR spectrum of copolymer MAA-CO-IAN and conjugates. A (copolymer MAA-CO-IAN), B (MAA-co-IAN-compound 1 conjugate), C (MAA-co-IAN-compound 2 conjugate), D (MAA-co-IAN-compound 3 conjugate)

The FTIR spectrum synthesis of copolymer (3; MAA-Co-IAN) with 3-((3-(4-aminophenoxy) phenyl) amino) -3, 4-dihydro-2H-thiazolo[3, 2-a][1, 3, 5]triazin-6(7H) -one is shown in Figure 6 D. It indicates absorption bands at 3415 cm^{-1} to OH overlapping with –NH stretching, 3174 cm^{-1} to C-H (aromatic), 2954 cm^{-1} to C-H (aliphatic), 1539 cm^{-1} to C=N, 613 cm^{-1} to C-S, 1510 cm^{-1} to C=C (aromatic), 1255 cm^{-1} to C-N, 1676 cm^{-1} to C=O (acid), 1643 cm^{-1} to C=O (amide), 1361 cm^{-1} to CH_3, and 1172 cm^{-1} to C-O.

^{1}H NMR spectrum of copolymer MAA-CO -IAN

Singlets occurred at (5.7 - 6.2 δ ppm) assigned to (4H, heterocyclic ring), a singlet at (12.5 ppm) assigned to –OH, a singlet at (2.5 ppm) assigned to –CH_3, and singlets at (3.3 ppm) assigned to –CH_2 (copolymer MAA-co-IAN). Furthermore, singlets occurred at (6.3 – 9.0 δ ppm) were assigned to (9H, phenyl ring), singlets at (3.4 ppm) assigned to –NH, singlets at (4.2-5.1 ppm) assigned to –NH (amide), a singlet at (11.5 ppm) assigned to (COOH), singlets at (2.5 ppm) assigned to –CH_2, and singlets at (1.0 ppm) assigned to –CH_3 (MAA-co-IAN-compound 1 conjugate). Also, singlets occurred at (6.5 - 8.3 δ ppm) assigned to (4H, phenyl ring), a multiplet at (3.3 ppm) assigned to -NH, multiple singlets at (5.2–5.6 ppm) assigned to -NH (amide), a singlet at 2.5 ppm assigned to CH_2, one at 1.0–1.1 ppm assigned to CH_3, and a singlet at 11.3 ppm assigned to OH (COOH; MAA-co-IAN-compound 2 conjugate). MAA-co-IAN-compound 3 conjugate exhibited signals at (6.5–8.3 δ ppm) for the (4H, phenyl ring), a singlet at (3.2 ppm) assigned to the -NH, a singlet at (4.5 ppm) assigned to the -NH (amide), a singlet at 2.5 ppm assigned to CH_2, one at 0.9 ppm assigned to CH_3, and a singlet at 11.3 ppm assigned to OH (COOH; Figure 7).

^{13}C-NMR spectrum of copolymer MAA-co-IAN

The C=O signal occurred at 198 ppm (ester), signal related to C=O (acid) at 178 ppm, signal related to CH_3 at 18 ppm, signal related to C-O at 76 ppm (copolymer MAA-co-IAN). Signals of olefinic and aromatic carbons appeared in the third region between 125 and 135 ppm; signals related to C-S at 56 ppm; signals related to C=N at 166 ppm, signal related to C-N at 64 ppm, signal related to C=O (amide) at 173 ppm, signal related to C=O (acid) at 182 ppm (MAA-co-IAN-compound 1 conjugate). Olefinic and aromatic carbon signals were seen in the third region, from 111 to 134 ppm; 56 ppm for a C-N signal; 164 ppm for a C=O (amide) signal; 200–205 ppm for a C=S signal; 180 ppm for a C=O (acid) signal; 18 ppm for a CH_3 signal; and 143 ppm for a C=N signal (MAA-co-IAN-compound 2 conjugate). Signals of aromatic and olefinic carbons appeared from 128 to 135 ppm. There were signals of C=N at 63 ppm; of C-S at 56 ppm; of C=O (amide) at 166 – 174 ppm; of C=O (acid) at 182 ppm; of CH_3 at 18 ppm. There was a single signal (MAA-co-IAN-compound 3 conjugate; Figure 8).

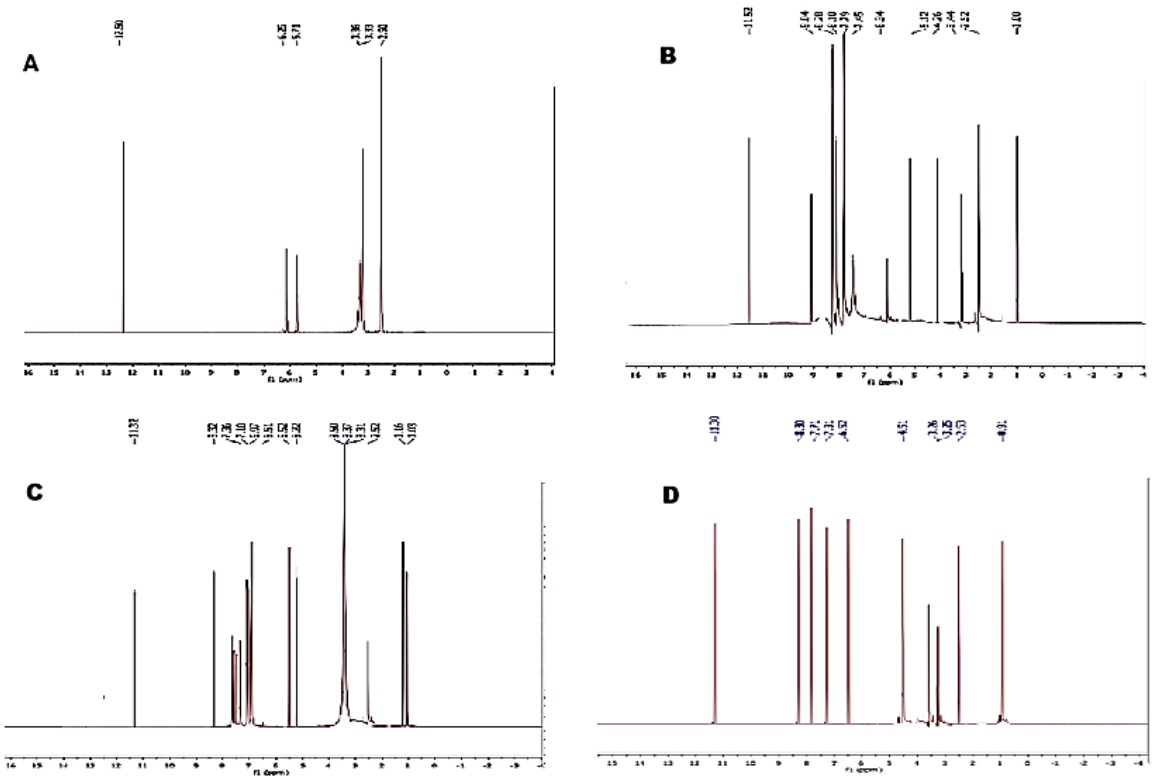

Figure 7: ^{1}HNMR spectrum of copolymer MAA-co-IAN (A), MAA-co-IAN-compound 1 conjugate (B) MAA-co-IAN-compound 2 conjugate (C), MAA-co-IAN-compound 3 conjugate (D)

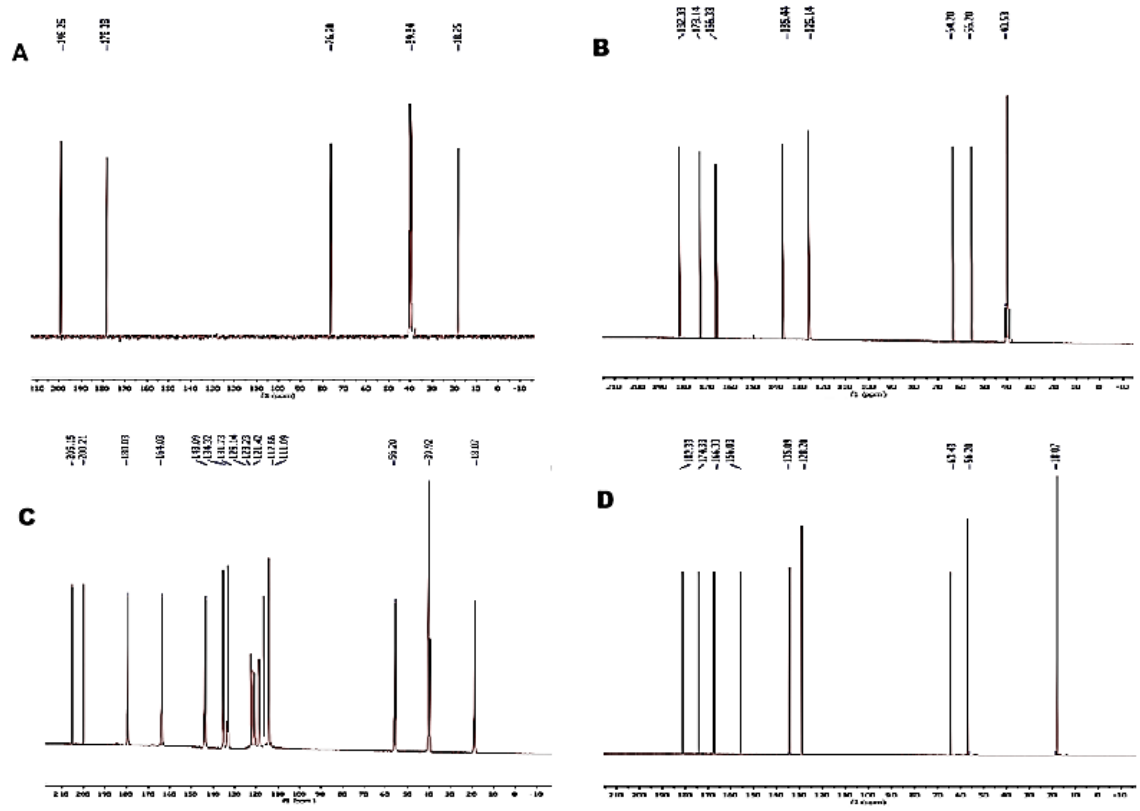

Figure 8: ^{13}C-NMR spectrum of copolymer MAA-co-IAN (A), MAA-co-IAN-compound 1 conjugate (B), MAA-co-IAN-compound 2 conjugate (C), MAA-co-IAN-compound 3 conjugate (D)

Cytotoxic evaluation of the compounds on colon cancer cell line (HCT-116)

Cytotoxic effects of compounds 1 to 3 were evaluated against HCT-116 colon cancer cells and HDFn normal cells at 25 – 400 µg/mL following 24, 48, and 72 h of exposure.

Cytotoxicity after 24 and 48 h

After 24 h, compound (1) reduced HCT-116 cell viability from 89.550 ± 0.306 % at 25 µg/mL to 39.978 ± 0.660 % at 400 µg/mL, while HdFn viability ranged from 97.880 ± 0.665 % to 82.742 ± 0.650 % over the same concentration range (Figure 9). The IC_{50} value for HCT-116 cells was 122.3 µg/mL (Figure 9 A). At 24 h, the HdFn was 311 µg/mL, and the HCT-116 IC_{50} was 145 µg/mL. Compound (2) reduced HCT-116 viability from 84.589 ± 0.421 % to 34.488 ± 0.683 % between 25 and 400 µg/mL, while HdFn viability decreased from 97.974 ± 0.649 % to 78.868 ± 0.394 % (Figure 9 B). Compound (3) similarly reduced HCT-116 viability from 87.040 ± 0.706 % to 36.981 ± 0.592 %, while HdFn viability decreased from 98.414 ± 0.221 % to 80.189 ± 0.515 %. The IC_{50} value of compound (3) against HCT-116 cells was 112.4 µg/mL (Figure 9 C). Following 48 h exposure, the cytotoxic effects increased across the concentration range. For compound (1), HCT-116 viability decreased from 87.013 ± 0.624 % at 25 µg/mL to 37.346 ± 0.432 % at 400 µg/mL, compared with 97.835 ± 0.172 % and 80.096 ± 0.373 %, respectively, in HdFn cells. The IC_{50} values were 108.3 µg/mL for HCT-116 and 199.4 µg/mL for HdFn cells (Figure 9 D). Compound (2) reduced HCT-116 viability from 81.323 ± 0.882 % to 30.400 ± 0.696 %, while HdFn viability decreased from 96.160 ± 0.481 % to 70.005 ± 0.753 % at 25 and 400 µg/mL, respectively (Figure 9 E). The corresponding IC_{50} values were 38.16 and 77.67 µg/mL for HCT-116 and HdFn cells, respectively. Compound (3) reduced HCT-116 viability from 83.873 ± 0.696 % to 34.176 ± 0.690 %, compared with 97.539 ± 0.017 % to 77.956 ± 0.577 % in HdFn cells. The IC_{50} values were 98.46 µg/mL for HCT-116 and 183.7 µg/mL for HdFn cells (Figure 9 F).

Cytotoxicity after 72 h

After 72 h, all three compounds reduced HCT-116 cell viability. Compound (1) reduced HCT-116 viability from 79.980 ± 0.895 % at 25 µg/mL to 32.348 ± 0.588 % at 400 µg/mL, while HdFn viability ranged from 94.969 ± 0.312 % to 74.878 ± 0.720 %. The IC_{50} values were 85.07 µg/mL for HCT-116 and 167.9 µg/mL for HdFn cells (Figure 10 A). For compound (2), HCT-116 viability decreased from 66.065 ± 0.509 % to 20.923 ± 0.512 %, whereas HdFn viability decreased from 91.747 ± 0.381 % to 61.297 ± 0.334 % over the same concentration range. The IC_{50} values were 50.62 µg/mL for HCT-116 and 124.0 µg/mL for HdFn cells (Figure 10 B). Compound (3) reduced HCT-116 viability from 71.923 ± 0.812 % to 28.311 ± 0.350 %, while HdFn viability decreased from 94.479 ± 0.286 % to 71.174 ± 0.464 % at 25 and 400 µg/mL, respectively. The corresponding IC_{50} values were 36.51 µg/mL for HCT-116 and 77.87 µg/mL for HdFn cells (Figure 10 C).

DISCUSSION

The FTIR spectra confirmed the successful formation of the synthesized derivatives, supporting the proposed chemical structures. The characteristic absorption bands corresponding to amino/amine, carbonyl, carboxylic acid, imine (C=N), thiocarbonyl (C=S), azo (N=N), C–N, C–S, C–O, and aromatic C–H functionalities indicated the presence of expected structural moieties. Broad high-frequency absorptions were associated with amino and amine groups, including intermolecular hydrogen bonding, while the observed aromatic and aliphatic C–H vibrations confirmed the retention of aromatic and polymeric segments following immobilization [9]. The simultaneous occurrence of these characteristic functional groups, particularly the nitrogen- and sulfur-containing functionalities, supports the incorporation of the intended heterocyclic moieties into the synthesized structures. The absence of significant unexpected absorption bands further suggests good reaction selectivity and an adequate degree of structural purity. Overall, the FTIR spectral profiles are consistent with the proposed structures and provide evidence that the intended cyclization and functionalization reactions occurred successfully, supporting further characterization and biological evaluation [9]. The infrared spectrum supported the successful synthesis of the target thiadiazole/thiazolo-triazine derivative.

The characteristic amino, hydroxyl, carbonyl, imine, and aromatic C–H/C=C absorption bands confirmed the presence of major functional groups proposed in the structure. The C–N, C–S, and C–O stretching vibrations further supported the formation of nitrogen- and sulfur-containing heterocyclic frameworks and ether functionalities. Overall, the observed spectral pattern was consistent with the proposed structure and indicated that the desired cyclization occurred under the experimental conditions [10].

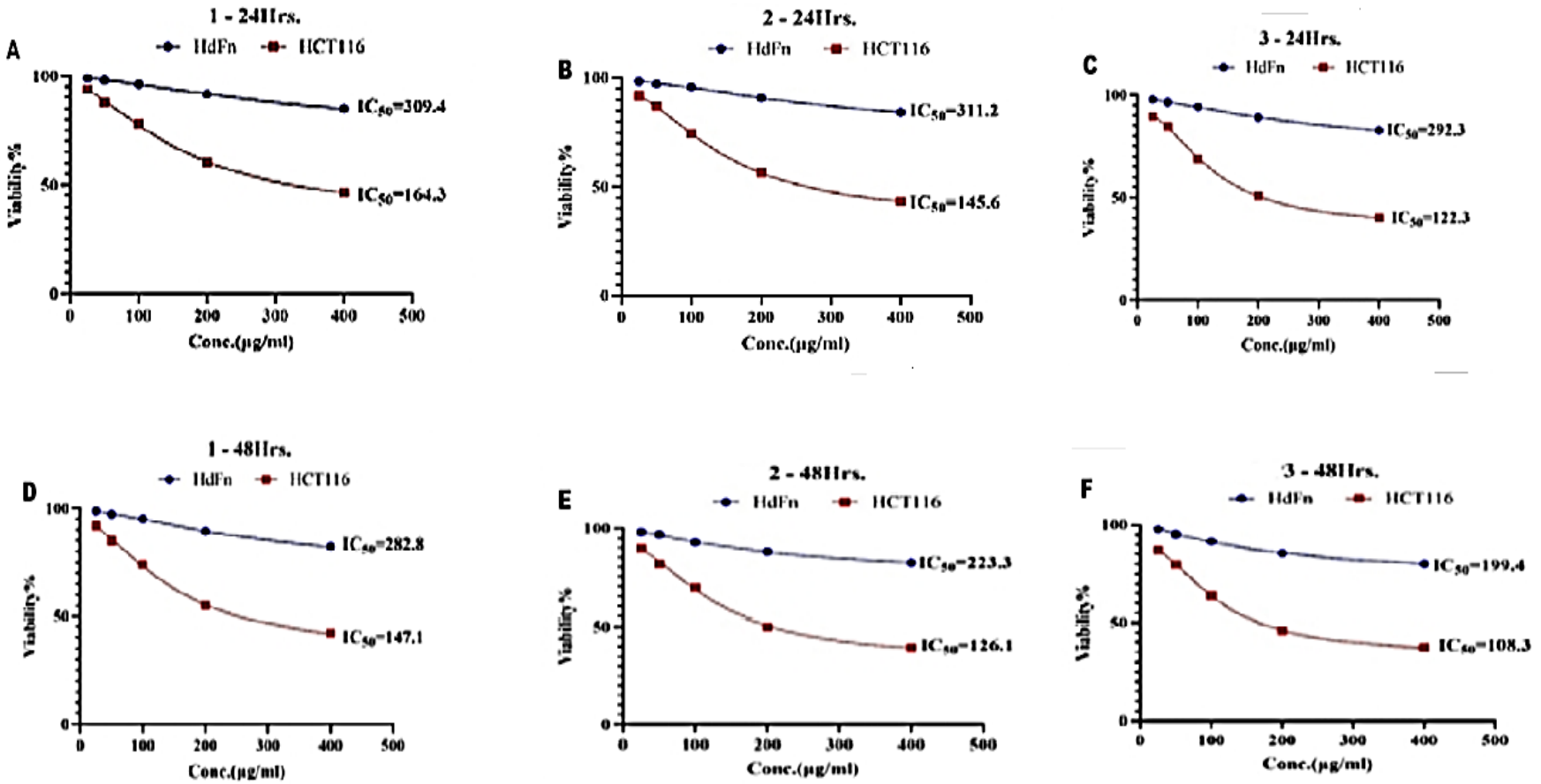

Figure 9: Cytotoxic potentials of compound 1 (A, D); compound 2 (B, E); and compound 3 (C, F) after 24 h and 48 h exposure, respectively

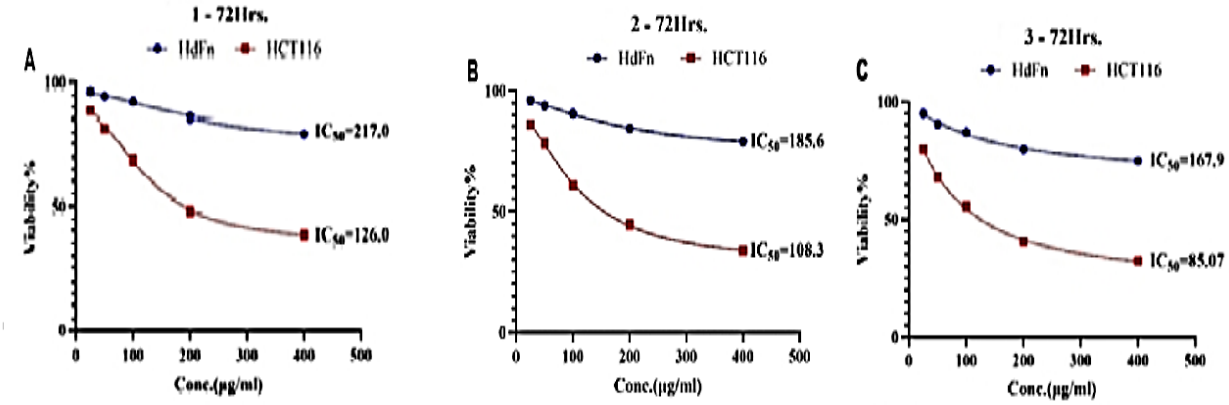

Figure 10: Cytotoxic potentials of compound 1 (A), compound 2 (B), compound 3 (C) on the colon cancer cell line compared to the normal cell line after 72 h at 37 °C

There was a concentration- and time-dependent decrease in cell viability for compounds (1–3), with greater reductions generally observed in HCT-116 cells compared to HdFn cells. The IC_{50} values of compound 2 increased from 38.16 to 50.62 µg/mL (HCT-116) and from 77.67 to 124.0 µg/mL (HdFn) between 48 and 72 h. Copolymer 2 remained the most potent compound, and its dominance became more pronounced at 48 h of exposure. At 400 µg/mL, the viability of HCT-116 cells decreased significantly to 30.40 ± 0.696 %, while HDFn cells retained a higher viability of 70.005 ± 0.753 %, representing the largest selectivity margin among all tested compounds. This superior activity is further confirmed by the IC_{50} values, which reached 38.16 µg/mL in cancer cells in comparison to 77.67 µg/mL in normal cells, indicating increased cytotoxic activity with prolonged exposure. Changes with increasing exposure time suggested that the compounds may initially interact with cellular targets and subsequently produce sustained intracellular effects that compromise cellular function and viability [11]. The differential response between normal HdFn and HCT-116 colon cancer cells further suggested that the physicochemical and structural characteristics of the compounds may influence cellular activity. Structural features of compound (1) may favour interactions with intracellular targets.

Naphthalimide- and related aromatic systems have been associated with DNA interaction, alteration of DNA topology and interference with topoisomerases, processes that may ultimately contribute to DNA damage, cell-cycle arrest and cell death [12,13]. Although Compound 1 contains isoindolinone/phthalimide-type structural units rather than a naphthalimide moiety, comparison with reported naphthalimide derivatives is considered relevant in the broader context of imide-containing heterocyclic compounds investigated for biological and anticancer activities. This comparison is based on their shared imide-related structural features and potential biological relevance, rather than on direct structural identity. The presence of sulfur-containing functionality may additionally contribute to redox-related effects and oxidative stress. As a result, the activity of compound (1) may involve a combination of intracellular molecular interactions and oxidative or metabolic stress. Compound (2) possesses a structurally complex, nitrogen- and sulfur-rich framework containing several heterocyclic features. The presence of multiple heteroatoms provides potential sites for hydrogen bonding, coordination and molecular interactions with intracellular targets.

Tetrazole-containing compounds have been investigated for their pharmacological and anticancer properties, including the potential to interact with cellular targets involved in apoptosis and cell-cycle regulation [14]. Structural characteristics of compound (2) may therefore support interactions with multiple intracellular targets, potentially affecting essential metabolic processes, redox balance and mitochondrial function. Compound (3) combines aromatic systems, heteroatoms and flexible polar linkages, providing a balance between hydrophobicity and polarity. Such structural balance may favour both membrane permeability and interactions with intracellular targets. The presence of sulfur-containing functionality may also contribute to redox activity and the generation of reactive oxygen species, which promote oxidative stress and mitochondrial dysfunction. As a result, the cytotoxic activity of compound (3) may involve sustained intracellular interactions and oxidative mechanisms [15]. Overall, the cytotoxic activity of

compounds 1 to 3 may be attributed to the combined influence of heterocyclic, aromatic, sulfur- and nitrogen-containing structural features. These characteristics may facilitate cellular uptake and interaction with intracellular targets and may promote processes such as oxidative stress, mitochondrial dysfunction, DNA interaction, enzyme inhibition, cell-cycle disruption and apoptosis. Compound-specific structural differences may account for variations in biological behaviour. Further mechanistic investigations are required to establish the precise pathways through which these compounds exert their cytotoxic effects and to assess their potential as anticancer agents [16].

CONCLUSION

The synthesized compounds and copolymers exhibit cytotoxic activity against colon cancer cell line (HCT-116), with responses influenced by concentration and duration of exposure. The findings provide a useful basis for further mechanistic studies, optimization, and evaluation of these compounds as potential candidates for pharmaceutical development.

DECLARATIONS

Acknowledgement/Funding

The authors gratefully acknowledge the support provided by the College of Pharmacy of the University of Babylon.

Use of Artificial intelligence/Large language models

The authors confirm that AI-based tools were used solely for language editing and manuscript polishing purposes (e.g., grammar, phrasing, and clarity). No AI tools were used to generate content, interpret data, or influence study design, results, or conclusions. All intellectual contributions, study analyses, and interpretations reported in the manuscript are the original work of the authors.

Availability of data and materials

The datasets used and/or analysed during the current study are available from the corresponding author on reasonable request.

Conflict of interest

The authors declare no conflict of interest.

Contribution of authors

We declare that this work was done by the author(s) named in this article, and all liabilities pertaining to claims relating to the content of this article will be borne by the authors.

REFERENCES

1. *Smith S, Goodge K, Delaney M, Struzyk A, Tansey N, Frey M. A comprehensive review of the covalent immobilization of biomolecules onto electrospun nanofibers. Nanomaterials 2020; 10(11): 2142. https://doi.org/10.3390/nano10112142.*
2. *Alsolami ES, Alorfi HS, Alamry KA, Hussein MA. One-pot multicomponent polymerization towards heterocyclic polymers: a mini review. RSC Adv 2024; 14(3): 1757-1781. doi: 10.1039/d3ra07278a*
3. *Alsolami ES, Alorfi HS, Alamry KA, Hussein MA. One-pot multicomponent polymerization towards heterocyclic polymers: a mini review. RSC Adv 2024; 14(3): 1757-1781. doi: 10.1039/d3ra07278a*
4. *Timofeeva L, Kleshcheva N. Antimicrobial polymers: mechanism of action, factors of activity and applications. Applied Microbiol Biotechnol 2011; 89(3): 475–492.*
5. *Alahari A, Trivelli X, Guérardel Y, Dover LG, Besra GS, Sacchettini JC, et al. Thiacetazone, an antitubercular drug that inhibits cyclopropanation of cell wall mycolic acids in mycobacteria. PLoS One 2007; 2(12): e1343. doi:10.1371/journal.pone.0001343*
6. *Bajaj K, Buchanan RM, Grapperhaus CA. Antifungal activity of thiosemicarbazones, bis(thiosemicarbazones), and their metal complexes. J Inorganic Biochem 2021; 225: 111620.*
7. *Korkmaz G. A review of recent research on the antimicrobial activities of thiosemicarbazone-based compounds. Journal of New Results in Sci 2024; 13(1): 61–83*
8. *da Cunha PST, Gini ALR, Chin CM, dos Santos JL, Scarim CB. Recent Progress in thiazole, thiosemicarbazone, and semicarbazone derivatives as antiparasitic agents against Trypanosomatids and Plasmodium spp. Molecules 2025; 30(8): 1788*
9. *Karakuş G. Derivatization of some maleic anhydride-containing copolymers with amine-functionalized pharmaceutical active substances, structural characterizations and biological activities. Marmara Pharm J 2015; 19(2): 121–125.*
10. *Mosmann T. Rapid colorimetric assay for cellular growth and survival: application to proliferation and cytotoxicity assays. J Immunological Methods 1983; 65(1–2): 55–63.*
11. *Ali NHO, Hamid MHSA, Putra NAM'A, Adol HA, Mirza AH, Usman A, et al. Efficient eco-friendly syntheses of dithiocarbazates and thiosemicarbazones. Green Chem Letters Rev 2020; 13(2): 129–140.*
12. *El-Metwaly NM, Alrefaei AF, Alshareef HF, Almehmadi SJ, Alotaibi FA, Alshammari NM, et al. Synthesis,*

characterization, molecular docking study and biological evaluation of novel 1,3,4-thiadiazole-based heterocycles as potential anticancer and antioxidant agents. Chem Biol Drug Design 2026; 108(1): e70361

13. Marullo R, Werner E, Degtyareva N, Moore B, Altavilla G, Ramalingam SS, et al. Cisplatin induces a mitochondrial-ROS response that contributes to cytotoxicity depending on mitochondrial redox status and bioenergetic functions. PLoS One 2013; 8(11): e81162. doi: 10.1371/journal.pone.0081162.
14. Singh I, Luxami V, Paul K. Synthesis of naphthalimide-phenanthro[9,10-d]imidazole derivatives: In vitro evaluation, binding interaction with DNA and topoisomerase inhibition. Bioorg Chem 2020; 96: 103631. doi:10.1016/j.bioorg.2020.103631
15. Tomczyk MD, Walczak KZ. 1,8-Naphthalimide-based DNA intercalators and anticancer agents. A systematic review from 2007 to 2017. Eur J Med Chem 2018; 159: 393–422. doi: 10.1016/j.ejmech.2018.09.055
16. Tandon R, Luxami V, Kaur H, Tandon N, Paul K. 1,8-Naphthalimide: A potent DNA intercalator and target for cancer therapy. Chem Rec 2017; 17(10): 956–993. doi: 10.1002/tcr.201600134
17. Popova EA, Protas AV, Trifonov RE. Tetrazole derivatives as promising anticancer agents. Anti-Cancer Agents Med Chem 2017; 17(14): 1856–1868. doi: 10.2174/1871520617666170327143148
18. Martins P, Jesus J, Santos S, Raposo LR, Roma-Rodrigues C, Baptista PV, et al. Heterocyclic anticancer compounds: recent advances and the paradigm shift towards the use of nanomedicine's toolbox. Molecules 2015; 20(9): 16852-16891. doi: 10.3390/molecules200916852